Nuclear Instruments and Methods in Physics Research A 598 (2009) 207–212

Contents lists available at ScienceDirect

Nuclear Instruments and Methods in Physics Research A

journal homepage: www.elsevier.com/locate/nima

New developments on photosensors for particle physics

D. Renker *

Paul-Scherrer-Institute, Villigen PSI, 5232 Villigen, Switzerland

ARTICLE INFO

Available online 15 August 2008

Keywords:
Photomultiplier tube
Hybrid photodiode
PIN photodiode
Avalanche photodiode
Geiger-mode photodiode
SiPM
VLPC

ABSTRACT

The needs of experiments in high-energy physics have been for many decades the stimulus for detector developments. For calorimetry, particle identification with ring image Cherenkov detectors, time-of-flight measurements, etc., sophisticated photosensors have been realized. Although photomultiplier tubes are a commercial product since 70 years, an impressive progress has been made recently. The bulky shape turned in a slim design and the quantum efficiency has been increased by almost a factor of 2. During the last 3 decades photodetectors made from semiconductor materials, photodiodes and avalanche photodiodes, have replaced in an increasing number the traditional photomultiplier tubes. The recently developed Geiger-mode avalanche photodiodes with high sensitivity to single photons will accelerate this trend.

1. Introduction

The detection of light is one of the key processes in experimental physics, from solid-state physics to high-energy physics and astroparticle physics. The energy of the particles to be observed is partly converted into visible photons which then are detected by appropriate sensors. In calorimeters made of scintillating crystals, liquid noble gases or plastic scintillators interleaved with dense materials like lead, the total energy of particles can be measured with good precision and a high dynamic range up to 10^5. The speed of particles can be determined by a measurement of the time-of-flight with very fast plastic scintillators and fast light sensors or by the measurement of the angle of Cherenkov light emitted when relativistic particles traverse transparent materials. With scintillating fibers the tracks of particles and, when there is a magnetic field, their momentum can be measured. Experiments with huge volumes of thousands of cube meters can be realized when Cherenkov light is produced and detected in water, ice or in the air of the atmosphere.

The first photodetector used in particle physics was the human eye. Rutherford and his co-workers watched the little light flashed produced on a phosphor screen where α-particles impinged after they scattered on the atoms of a gold foil [1].

In the year 1913 Elster and Geitel invented the first photoelectric tube. In 1889, they had reported the photoelectric effect induced by visible light striking an alkali metal [2]. In 1930 the first photomultiplier tube (PMT) was invented by Kubetsky. In 1939 Zworykin and Rajchman [3] from the RCA laboratories developed a PMT with electrostatic focusing, the basic structure of current PMT's, and a short time after it became a commercial product. Single photons were detectable from now on. Further innovations have led to highly sophisticated devices available nowadays.

Hybrid photodetectors are a variant of the photomultiplier. The vacuum container and the photocathode are the same but the multiplication is not done in a chain of dynodes. The electrons liberated in the photocathode by a photon are accelerated in a high electric field (15–25 kV) and are focused onto a silicon diode or onto an avalanche photodiode (APD). In the silicon the electrons lose their energy by ionization, they produce electron–hole pairs which can be collected. In average an energy of 3.6 eV is needed to create one electron–hole pair. This defines the amplification which is some 5000 (10^5–10^6 when an APD is used).

Both, normal and hybrid PMTs, are extremely sensitive to magnetic fields. Only some specialized devices work in magnetic fields but only if it is strictly axial.

General purpose detectors need magnetic fields for the measurement of the momentum of charged particles. The PMTs had to be replaced by solid-state devices. Although the p–n junction of solid-state photodiodes had been discovered already in 1939 by Russel Ohl [4] not earlier than in the 1980 the improved purification and growing processes made them suitable for particle physics experiments and the L3 collaboration was the first to propose the use of the so-called PIN photodiodes in big numbers [5]. Then the development was relatively fast: in the early 1990 the APDs with internal gain became a commercial product and soon the CMS experiment adopted them for the electromagnetic calorimeter [6]. In parallel, the metal resistive structures of silicon diodes has been developed in Russia which led to the Geiger-mode APDs (G-APDs). Pioneers were Golovin [7] and Sadygov [8]. Basic work on the theory of solid-state single

* Tel.: +41 56 3104213; fax: +41 56 3105230.
E-mail address: dieter.renker@psi.ch

0168-9002/$ - see front matter © 2008 Elsevier B.V. All rights reserved.
doi:10.1016/j.nima.2008.08.023

photon detectors was done by McIntyre at RCA [9] and by Haitz in the Shockley research laboratory [10] already in the 1960.

In the Rockwell International Science Center, Stapelbroek et al. in 1987 developed the solid-state photomultiplier (SSPM). This is an APD with very high donor concentration which creates an impurity band 50 meV below the conducting band. Later this device was modified to be less sensitive to infrared light and is now called visible-light photon counter (VLPC). The small band gap forces an operation at very low temperatures of few degree Kelvin [11].

Gaseous detectors were for a long time based on photo-conversion in gas and subsequent photoelectron charge multiplication in a gas avalanche. Large areas have been covered and no other technique is cost competitive but they had principle difficulties: ion- and photon-feedback. Nowadays, the photosensitive vapors have been replaced by solid CsI photocathodes and the ion- and photon-feedback is suppressed by the use of the gas electron multiplier (GEM) foils which were invented in 1997 by Sauli [12].

Most emphasis will be given in this article to G-APDs which are relatively new and very promising.

2. Photomultiplier tube (PMT)

PMT's can be fabricated with large sensitive areas. The biggest are the tubes with 50 cm diameter used in the SuperKamiokande experiment.

The gain of PMTs is 10^6–10^7 and the output signal can be processed without additional amplification in standard electronic circuits. The amplification in the dynodes of a PMT has an extremely low level of noise. Rare and weak light flashes can therefore be detected without getting overloaded by noise events. Summing over a large number of coincident PMT signals is possible. The so-called Muegamma experiment at PSI aims to measure the decay $\mu^+ \to e^+ + \gamma$ with a sensitivity better than 5×10^{-14}. The γ's will be detected in a 800 l liquid xenon calorimeter by the observation of the scintillation light with 800 PMT's. The deposited energy will be derived from the sum of all PMT signals and the position of the γ conversion will be calculated from the distribution of the individual amplitudes [13].

Some specialized PMTs have a very small transition time spread and the time resolution that can be achieved with these devices is very good. With fine mesh PMTs from Hamamatsu in the time-of-flight detector with 300 cm long scintillator bars of BELLE the resolution is better than 100 ps [14] and in the KLOE calorimeter with 430 cm long fibers it is $54\,\mathrm{ps}/\sqrt{E(\mathrm{GeV})} \oplus 50\,\mathrm{ps}$ [15]. The fine mesh PMTs work in axial magnetic field.

Although the PMTs are a commercial product since 70 years the recent progress is remarkable: the bulky shape turned into a flat design with very good effective area coverage.

PMTs became position sensitive when the single dynode chain was replaced by the so-called metal-channel structure [Hamamatsu H9500] or by micro-channel plates [Burle Planacon] and a segmented (pixelized) anode.

A real surprise came in 2006/2007 when two companies, Photonis [16] and Hamamatsu [17], announced PMTs with the usual bialkali photocathode but with a quantum efficiency (QE) almost twice higher than that of a standard device (Fig. 1). This was achieved by going to ultra-pure photocathode materials (99.9999%) and a fine tuning of the deposition process.

A new material for the photocathode is GaAsP which promises a QE of ~45% but it is difficult to produce and the price is high.

3. Hybrid photodiode (HPD)

HPDs have excellent sensitivity and resolution for single photons (Fig. 2). Only the unavoidable backscattering of electrons from the silicon diode reduces the response and causes crosstalk in position sensitive devices.

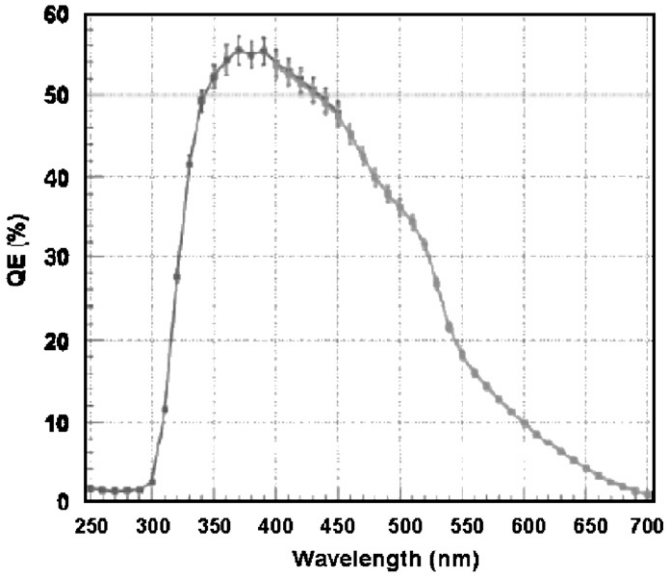

Fig. 1. Quantum efficiency of a "superbialkali" PMT from Photonis.

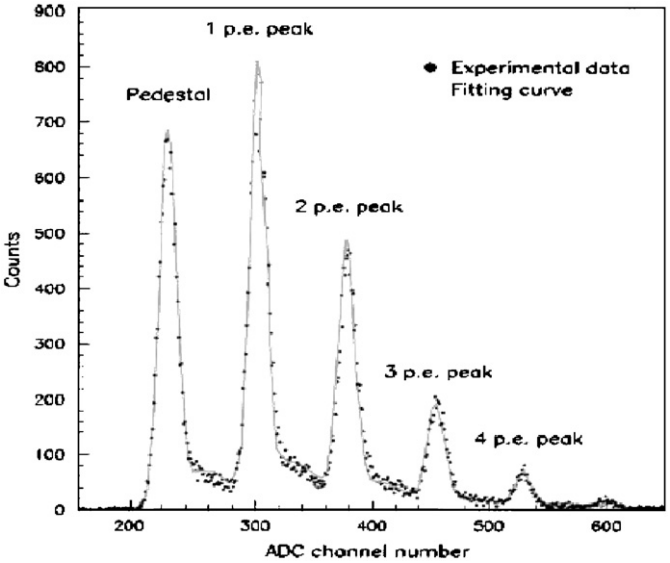

Fig. 2. Typical photoelectron spectrum for weak light flashes recorded from a full-scale prototype HPD operated at 20 kV. From Ref. [19].

State of the art is HPD of the ring image Cherenkov detector for particle identification in LHCb. The electrons are focused with a $5\times$ demagnification onto a pixelized silicon diode with 8192 channels organized in 1024 super-pixels of $500 \times 500\,\mu\mathrm{m}^2$ size. The result is the desired granularity of $2.5 \times 2.5\,\mathrm{mm}^2$ [18].

4. PIN photodiode

One of the simplest kind of photodiodes is the PIN (or p–i–n) photodiode in which an intrinsic piece of semiconductor is sandwiched between two heavily doped n+ and p+ regions [20]. It is produced by standard semiconductor processes: boron diffusion on one side and phosphor diffusion on the other side of a high-purity silicon wafer. This configuration produces a field which, even without an external field supplied, will tend to

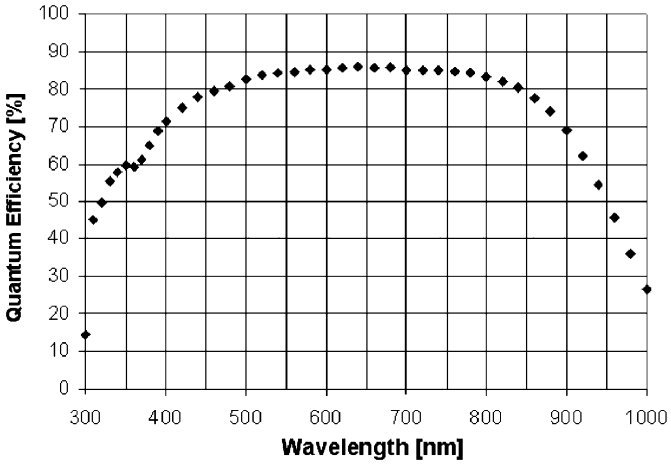

Fig. 3. Quantum efficiency of a PIN diode plotted over the wavelength.

separate charges produced in the depleted region. The separated charges will be swept to the terminals and detected as current provided that they are not recombined. The thick layer of intrinsic silicon (300 μm) reduces the capacity of the diode and by this the noise and makes it sensitive to red and infrared light which has a rather long absorption length in silicon.

A calorimeter made of CsI(Tl) crystals and a PIN photodiode readout was first built by CLEO [21]. CsI(Tl) has a light yield which is even higher than that of NaI(Tl) but the emission peaks at 550 nm. Photodiodes have at this wavelength a QE ~80% (Fig. 3) while PMT's have less than 10%. The detectors at the B-factories BELLE and BABAR have the same type of calorimeter and all achieve an energy resolution better than 2% for photons with an energy of 1 GeV.

The smallest detectable light flash needs to consist of several hundred photons because the device has no internal gain and a charge sensitive amplifier is needed which introduces noise to the system and makes the signal slow.

The full thickness of the PIN photodiodes (300 μm) is sensitive. Charged particles (e.g. e+ and e−) which leak out at the rear end of the crystals and pass the diode produce an unwanted addition to the signal, the so-called nuclear counter effect. A minimum ionizing particle (MIP) creates some 100 electron–hole pairs per micrometer in silicon. This makes 30 000 electron–hole pairs which fake ~2 MeV additional energy in a CsI(Tl) calorimeter and much more when a less efficient scintillator like $PbWO_4$ is used.

5. Avalanche photodiode (APD)

An APD provides gain due to the high internal field at the junction of positive and negative doped silicon. The electrons gain enough energy in this field that they can create by impact ionization a second free electron which then makes a third-an avalanche starts. The multiplication is moderate between 50 and 200. A gain of 10^4 is possible but at values higher than a few hundred the environment (e.g. temperature and voltage supply) needs to be extremely stable.

The size of APDs is limited due to the production yield. The biggest area available commercially is 2.5 cm^2.

Electrons produced in the p-layer of 5 μm thickness (Fig. 4) by photo-conversion or by ionising particles induce avalanche amplification at the p–n junction. Electrons created in the bulk by ionising particles are collected but not amplified. The net effect for a traversing MIP can be expressed by an effective thickness which is ~6 μm in the case of the APD developed for the CMS

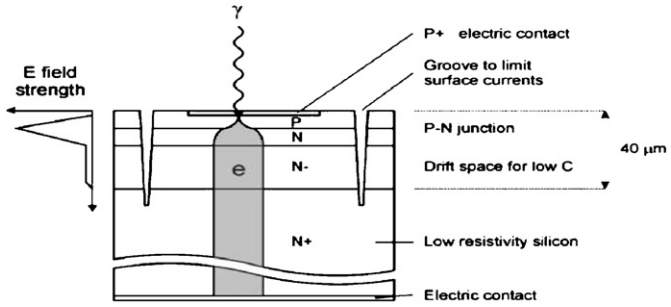

Fig. 4. Structure of the APD used by CMS.

electromagnetic calorimeter [22]. The nuclear counter effect is about 50 times smaller than in a PIN diode.

5.1. Stability

Compared to PIN photodiodes, the APDs are faster and due to their internal gain they are less sensitive to coherent noise but they contribute to all three terms of the energy resolution while the PIN photodiode influences only the statistic and the noise term. The statistic term is increased in addition to the effect of the QE, which is the same as for PIN diodes, due to the excess noise factor which describes the avalanche fluctuations. The sensitivity of the gain to voltage and temperature variation contributes to the constant term and the capacitance, serial resistance and dark current effect the noise term.

The excess noise factor F, the relative change of the gain M with the bias voltage $1/M^*dV/dM$ and the temperature $1/M^*dT/dM$ increase linearly with the gain [23]. Therefore, the CMS collaboration decided to operate the APDs at the relative small gain of 50.

6. Geiger-mode avalanche photodiode (G-APD)

A normal APD can be operated in Geiger-mode with a bias voltage above the breakdown voltage but the dark counts and the dead time and recovery time after a breakdown allow only areas with a diameter of some 100 μm. When larger areas are needed, the solution is to subdivide the area of a large APD into many cells and connect them all in parallel via an individual limiting resistor. The resulting devices we call G-APDs. They have similar properties as PMTs and some people call them therefore silicon photomultiplier, SiPM (more names are in use: MAPD, MPPC, SSPM, etc.).

Areas up to $5 \times 5\,mm^2$ are available.

G-APDs work at low bias voltage (<100 V), have low power consumption ($<50\,\mu W/mm^2$), are insensitive to magnetic fields up to 15 T, are compact, rugged, show no aging and tolerate accidental illumination.

6.1. Gain

The discharge currents from all cells (A_i) are added on a common load resistor and the output signal of a G-APD is the sum of the signals from all the cells firing at the same time (A). Globally seen the G-APD becomes in this way an analog device:

$$A_i \sim C\Delta V = C(V_{bias} - V_{breakdown})$$

C is the capacitance of 1 cell

$$A = \sum A_i.$$

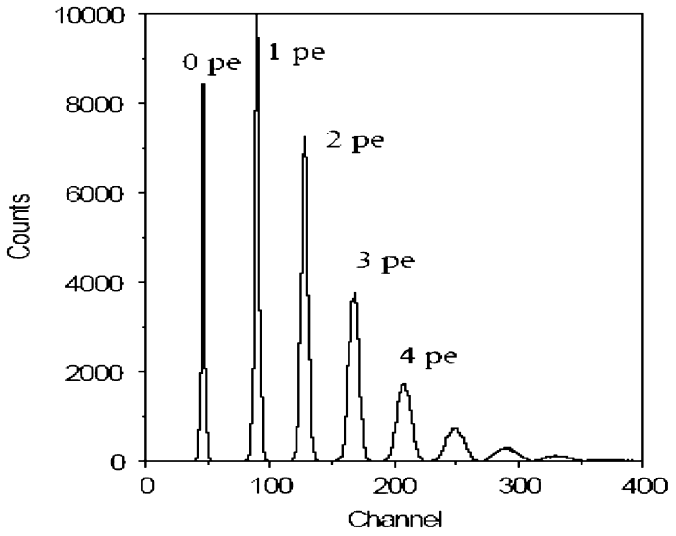

Fig. 5. Pulse height spectrum measured with a G-APD. Taken from Ref. [24].

The gain is in the range of 10^5–10^7. Since the cells act as individual photon counters without fluctuations in the signal amplitudes an excellent resolution for single photons can be achieved (Fig. 5). The excess noise factor is very small, could eventually be one. Some types of G-APDs show big deviations from this behavior because of a cell-to-cell crosstalk (see discussion below).

Like in a normal linear APDs, the gain strongly depends on variations of the bias voltage and of the temperature.

6.2. Linearity of the response

The high density of cells (100–10,000 per mm^2 are available) makes the response of a G-APD linear over a wide range of light intensities. The limits are due to the finite number of cells because two or more photons that impinge on 1 cell produce exactly the same signal as one single photon

$$N_{\text{firedcells}} = N_{\text{total}}(1 - \exp(-N_{\text{photon}}\text{PDE}/N_{\text{total}}))$$

where N_{photon} is the number of impinging photons and PDE is the photon detection efficiency of the G-APD. The finite number of cells N_{total} results in a deviation from linearity of the G-APD signals with increasing light intensity. When 50% of the cells fire at the same time the deviation from linearity is about 20%.

6.3. Photon detection efficiency (PDE)

The PDE of a G-APD is wavelength dependent

$$\text{PDE}(\lambda) = \text{QE}(\lambda)\, \varepsilon_{\text{geometry}}\, \varepsilon_{\text{Geiger}}(\lambda)$$

where $\text{QE}(\lambda)$ is the quantum efficiency (typically 80% for the whole wavelength range of visible light), $\varepsilon_{\text{geometry}}$ is the so-called geometrical efficiency, that is the fraction of the total G-APD area occupied by active cell areas and $\varepsilon_{\text{Geiger}}(\lambda)$ is the probability for a carrier created in the active cell volume to initiate a Geiger-mode discharge. The later strongly depends on the applied bias voltage and the wavelength of the light. The geometrical efficiency, limited by the dead area around each cell, depends on the construction and ranges typically between 40% and 80% of the total area.

Electrons have in silicon a higher probability to trigger a breakdown than holes. Therefore, the creation of free carriers in the p-layer of the G-APD has the highest probability to initiate a discharge. Devices which are made of p-silicon on a n-substrate are sensitive to blue light which is absorbed in silicon within a fraction of a micrometer. In devices with n-silicon on a p-substrate the light has to pass through the n-layer and only light with a wavelength longer than 500 nm has an absorption length of more than 1 μm. The PDE consequently peaks around 600 nm. In both types of G-APDs the maximal PDE can be higher than 60% either for blue or red light.

6.4. Recovery time

After a cell of a G-APD was discharged in a breakdown it has to be recharged via the individual quenching resistor. Some devices have a resistor with several MOhm which leads to a rather long recovery process. During this time the amplitude of an event in the same cell is reduced as well as the PDE due to a reduced triggering probability.

6.5. Dark counts

G-APDs produce dark counts with a rate that can exceed 1 MHz/mm^2. These dark counts are initiated by thermal generation or field-assisted generation (tunneling) of free carriers. The first and dominant effect can be reduced by cooling. The rate reduces in first order by a factor of 2 for every 8 °C. Only the operation at smaller bias voltage which leads to reduced gain and PDE effects the tunneling.

The count rate falls dramatically with an increasing threshold of the readout electronic. Each increase of the threshold by the equivalent of the 1 photoelectron amplitude reduces the count rate by almost one order of magnitude (Fig. 6). When the threshold is set to a value higher than the 4 photoelectron amplitude the dark count rate is below 1 Hz.

6.6. Crosstalk

During the breakdown of a cell of a G-APD a micro-plasma is formed and electrons are lifted to high bands. When they relax photons are emitted (~3 for 10^5 carriers traversing the p-n junction) [25]. These photons can travel to a neighboring cell and trigger a breakdown there. This photon-assisted crosstalk between the cells has a small but not negligible contribution to the G-APD output signals and, since it is a stochastic process, contribute to the excess noise factor which is increased to values between 1.1 and 1.3. The crosstalk can be eliminated almost

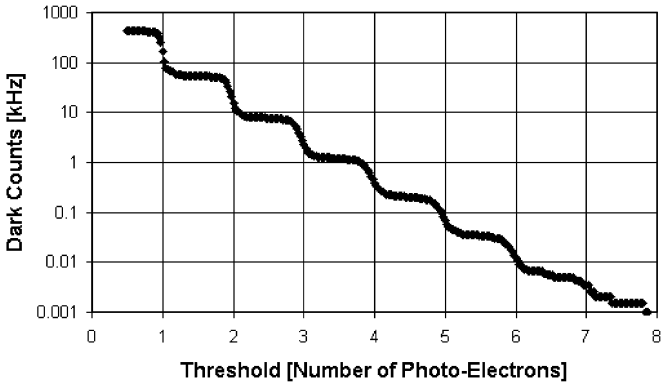

Fig. 6. Dark count rate for different values of the discriminator threshold. The G-APD used in this measurement is S10362-11-050C from Hamamatsu.

completely by an optical isolation in trenches between the cells but this needs space and reduces the overall PDE.

6.7. Afterpulses

In a breakdown with its local high current deep traps in the silicon are filled with carriers which are subsequently released. The time constant of the delayed release is typically 200–300 ns dependent on the temperature.

Afterpulses with short delay contribute little because the cells are not fully recharged but have an effect on the recovery time.

6.8. Time resolution

The active layers of silicon in a G-APD are very thin (2–4 μm), the avalanche breakdown process is fast and the signal amplitude is big. We can therefore expect very good timing properties even for single photons. A resolution of ~100 ps FWHM has been achieved for single photons (Fig. 7) [24].

The tail to the right of the distribution in Fig. 5 is caused by carriers which are generated in a field free region. They have to move first by diffusion. It can take several tens of nanoseconds until they reach a region with field, drift to the p–n junction and finally trigger a breakdown.

7. Visible light photon counter (VLPC)

VLPCs have like HPDs and G-APDs an excellent sensitivity and resolution for single photons. They are fast and insensitive to magnetic fields but have to be operated at cryogenic temperatures. D0 is the only experiment that uses these devices in big numbers for the central fiber tracker which consists of 80,000 fibers, 2.5 and 1.7 m long. The light produced by charged particles crossing a fiber is transported via ~10 m long optical fibers to VLPCs housed in a cryostat which regulates the operation temperature (6–8 K). Few photons arrive at the photodetector which therefore needs to have high QE of some 80% and single photon detection capability (Fig. 8) [26].

8. Gaseous detectors

The development of gas-filled detectors made enormous progress thanks to the invention of the gas electron multiplier

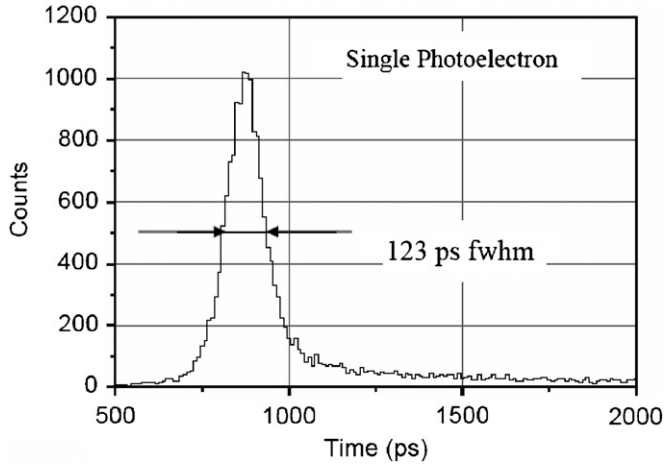

Fig. 7. Time resolution for single photons. The contribution from the laser and the readout electronic is ~40 ps.

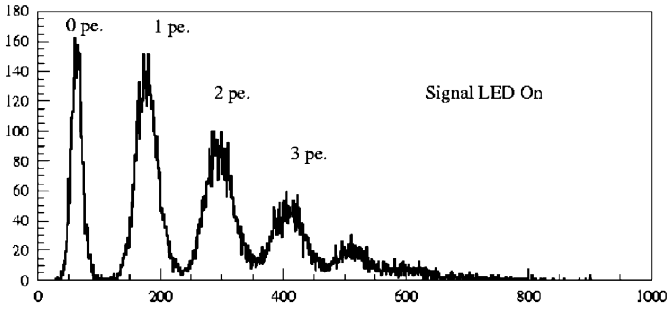

Fig. 8. Typical pulse height distribution from a VLPC illuminated with weak signals from a LED.

(GEM) fail [12]. In recent devices the photon feedback has been successfully suppressed and the ion back flow has been reduced to a very low level [27].

At moderate cost large area detectors can be built with sub-millimeter localization accuracy and a time resolution better than 1 ns. Gaseous detectors are sensitive to single photons in the spectral range from UV to visible light and the operation in high magnetic fields is possible.

They have high gain (several 10^5) and even so a long life time. See the contribution of Breskin to this issue.

9. Conclusion

A large variety of photosensor techniques has been developed and integrated in present detectors for particle physics. There is an almost infinite number of alternative designs which have been proposed and partly tested in prototypes.

Vacuum devices (PMTs and HPDs) recently have been improved considerably. Still they are the working horse when weak light flashes need to be detected.

Solid-state device are making very fast advance due to enormous progress in the processing of silicon. The PIN diode became a very successful device. It is used by most big general purpose detectors. CMS is the first big experiment that utilizes APDs which are the best choice when a high dynamic range is essential together with a low threshold. The new G-APDs allow a fast detection of very week light flashes down to single photons. They will for sure have a heavy impact on the design of future detectors.

New types of photo sensors are always quickly being adopted in particle physics experiments.

References

[1] E. Rutherford, Philos. Mag. Ser. 6 (21) (1911) 669;
H. Geiger, E. Marsden, Proc. R. Soc. 82A (1909) 495.
[2] J. Elster, H. Geitel, Ann. Phys. 38 (1889) 497.
[3] V.K. Zworykin, J.A. Rajchman, Proc. IRE 27 (1939) 558.
[4] Light Sensitive Device, US Patent 2402662.
[5] J.A. Bakken, et al., Nucl. Instr. and Meth. A 254 (1987) 535.
[6] G. Alexeev, et al., Nucl. Instr. and Meth. A 385 (1997) 425.
[7] V. Saveliev, V. Golovin, Nucl. Instr. and Meth. A 442 (2000) 223.
[8] P.P. Antich, et al., Nucl. Instr. and Meth. A 389 (1997) 491.
[9] R.J. McIntyre, J. Appl. Phys. 32 (6) (1961) 983.
[10] R.H. Haitz., J. Appl. Phys. 35 (5) (1964) 1370.
[11] M.R. Wayne, Nucl. Instr. and Meth. A 387 (1997) 278.
[12] F. Sauli, Nucl. Instr. and Meth. A 386 (1997) 531.
[13] A. Baldini, et al., Nucl. Instr. and Meth. A 545 (2005) 753.
[14] E. Nakano, Nucl. Instr. and Meth. A 494 (2002) 402.
[15] A. Antonelli, et al., Nucl. Instr. and Meth. A 370 (1996) 367.
[16] R. Mirzoyan, MPI Munich, Private Communication.
[17] Hamamatsu Data Sheet UBA_SBA_TPMH1305E01.pdf.
[18] S. Amato, et al. (LHCb Collaboration), CERN LHCC 2000-037.
[19] E. Albrecht, et al., Nucl. Instr. and Meth. A 442 (2000) 164.

[20] K. Yamamoto, et al., Nucl. Instr. and Meth. A 253 (1987) 542.
[21] E. Blucher, et al., Nucl. Instr. and Meth. A 249 (1986) 201.
[22] Th. Kirn, et al., Nucl. Instr. and Meth. A 387 (1997) 199.
[23] K. Deiters, et al., Nucl. Instr. and Meth. A 461 (2001) 574.
[24] P. Buzhan, et al., Nucl. Instr. and Meth. A 504 (2003) 48.
[25] A. Lacaita, et al., IEEE TED 40 (3) (1993) 577.
[26] A. Bross, et al., Nucl. Instr. and Meth. A 477 (2002) 172.
[27] A. Breskin, et al., Nucl. Instr. and Meth. A 553 (2005) 46.